Yukon River Discharge Response to Seasonal Snow Cover Change

9

Daqing Yang, Yuanyuan Zhao, Richard Armstrong, Mary J. Brodzik, and David Robinson

Abstract

We used remotely sensed Snow Water Equivalent (SWE) and Snow Cover Extent (SCE) data to investigate streamflow response to seasonal snow cover change over the Yukon watershed. We quantified the seasonal cycles and variations of snow cover (both SWE and SCE) and river streamflow, and identified a clear correspondence of river discharge to seasonal snow cover change. We also examined and compared the weekly mean streamflow with the weekly basin SWE and SCE. The results revealed a strong relationship between streamflow and snow cover change during the spring melt season. This relationship provides a practical procedure of using remotely sensed snow cover information for snowmelt runoff estimation over the large northern watersheds.

D. Yang (✉)
Watershed Hydrology and Ecology Division, Environment and Climate Change Canada, Victoria, BC, Canada
e-mail: Daqing.Yang@canada.ca; daqing.yang@gmail.com

Y. Zhao
Department of Mathematics and Statistics, University of Alaska Fairbanks, Fairbanks, AK 99775, USA
e-mail: yuanyuanzhao17@gmail.com

R. Armstrong · M. J. Brodzik
National Snow & Ice Data Center/CIRES, University of Colorado, Boulder, CO 80309-0449, USA
e-mail: rlx@nsidc.org

M. J. Brodzik
e-mail: brodzik@nsidc.org

D. Robinson
Department of Geography & NJ Agricultural Experiment Station, Rutgers University, Piscataway, NJ 08854-8054, USA
e-mail: david.robinson@rutgers.edu

D. Yang and D. L. Kane (eds.), *Arctic Hydrology, Permafrost and Ecosystems*,
https://doi.org/10.1007/978-3-030-50930-9_9

Analyses of extreme (high/low) streamflow cases (years) and basin snow cover conditions indicate an association of high (low) flood peak with high (low) maximum SWE. Comparative analyses of weekly basin SWE versus SCE, peak snowmelt floods, and climatic variables (temperature and winter precipitation) show consistency among basin SWE, SCE, and temperature, but there is some incompatibility between basin SWE and winter precipitation. The inconsistency suggests uncertainties in determination of basin winter snowfall amounts and limitations in applications of the SWE retrieval algorithm over large watersheds/regions with different physical characteristics. Overall, the results of this analysis demonstrate that the SWE and SCE data/products derived from remote sensing technology are useful in understanding seasonal streamflow variations in the northern regions.

9.1 Introduction

River discharge is an important element of freshwater budget for the Arctic Ocean and the high-latitude seas. The amount and variation of this freshwater inflow critically affect the salinity and sea ice formation, and may also exert significant control over global ocean circulation (Aagaard and Carmack 1989). Snow cover is a main component of global cryosphere system. Snow cover significantly affects atmosphere, hydrology, permafrost, and ecosystem in the high-latitude regions. Snow cover melt and associated floods are the most important hydrologic event of the year in the northern river basins (Woo 1986; Kane et al. 2000). Recent investigations document snowmelt has started earlier over the recent decades in the northern regions, such as Canada, Alaska, and Siberia, associated with warming in winter and spring seasons (Brabets et al. 2000; Serreze et al. 2000; Whitfield and Cannon 2000; Lammers et al. 2001; Zhang et al. 1999; Ye et al. 2003; Yang et al. 2002, 2014a, b). Studies also demonstrate that the timing and magnitude of northern river streamflow are strongly allied with cold season snow cover storage and subsequent melt (Cao et al. 2002; Yang et al. 2003, 2007). The changes in snowmelt runoff pattern may indicate a hydrologic regime shift over the high latitudes (Serreze et al. 2002; Yang et al. 2002, 2014a, b).

Snow depth data have been routinely collected at the operational networks in the United States and Canada. As a result of differences and changes in methods of observations and data-processing procedures, these data are subject to uncertainties and inconsistency over time and space, particularly across national borders. The operational networks in the northern regions are very sparse. It is therefore a challenge to combine regional snow data to generate basin snow information or gridded products for the high-latitude regions or large watersheds (Robinson 1989; Dyer and Mote 2006). Dyer (2008) used snow depth and discharge data to analyze patterns of snow volume and discharge in major North American watersheds (including the Yukon basin), and found, through statistical analysis, that snow

accumulation during late fall and winter is useful to predict spring discharge particularly in the cold Yukon basin and Mackenzie watersheds. Dyer (2008) pointed out that Snow Water Equivalent (SWE) and snow density data should be used to better define the snow accumulation and melt processes; however, reliable SWE and density estimates are difficult to obtain, especially for the continental-scale watersheds in the northern regions. Our knowledge of large-scale snowmelt processes and their interaction with climatic change and variation is incomplete, particularly for the northern regions with insufficient ground-based observations. This limits our ability of understanding past changes and predicting future characteristics of the hydrology system under a warming climate in the high-latitude regions.

Remotely sensed snow data have been very useful to cold region climate and hydrology investigations. For instance, the NOAA weekly snow cover dataset (maps) over the Northern Hemisphere permits quantitative assessments of changes and variations in regional snow extent (Robinson et al. 1993; Serreze et al. 1993; Clark et al. 1997; Frei and Robinson 1999b; Robinson and Frei 2000), and they are useful for hydrologic and snowmelt runoff models (Rango 1996, 1997; Rango and Shalaby 1999). Yang et al. (2003) used the weekly NOAA Snow Cover Extent (SCE) data to study streamflow hydrology in the large Siberian rivers, and discovered that SCE could predict spring discharge with the acceptable accuracy. In addition, long-term SWE data have been derived from the passive microwave sensors (Chang et al. 1987; Chang 1997; Armstrong and Brodzik 2001, 2002). Their potential utility for large-scale hydrology and climate studies in the high-latitude regions has not been fully evaluated. This chapter assesses the compatibility of the passive microwave SWE data over the Yukon watershed, and examines the streamflow response to snow cover change particularly during the spring melt season. The objective is to determine the potential of using remotely sensed snow cover information to enhance our capability of snowmelt runoff modeling over the large northern regions with continuous and discontinuous permafrost. Changes in seasonal snow cover conditions may have significantly contributed to the ground surface temperature increase. The influence of seasonal snow cover on soil temperature, soil freezing, thawing processes, and permafrost has considerable impact on carbon exchange between the atmosphere and the ground and on the hydrologic cycle in cold regions/cold seasons (Zhang 2005). The methods and results of this analysis should improve our understanding of hydrologic effects of a shrinking cryosphere.

9.2 Basin, Datasets, and Methods

The Yukon has a drainage area of 840 000 km^2. It is 3185-km long, with 1149 km in Canada. The Yukon River rises from the Atlin Lake and flows northwest to Fort Yukon, and then turns southwest and enters the Bering Sea (Fig. 9.1). Its major tributaries are the Teslin, Pelly, White, Stewart, Porcupine, Tanana, and Koyukuk rivers. The Yukon basin consists of 37% rolling topography and gentle slopes, 24%

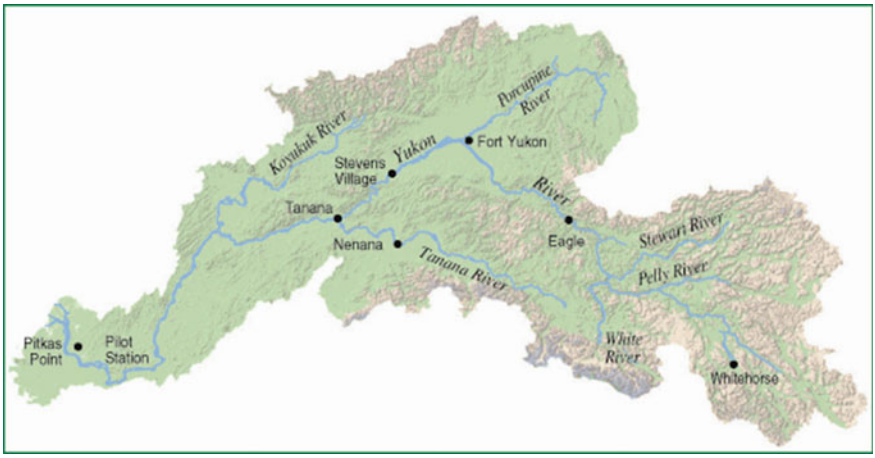

Fig. 9.1 The Yukon River basin and its tributaries

low mountains 20% plains and low mountains, 17% moderately high rugged mountains, and 2% extremely high rugged mountains. The Yukon River is one of the largest rivers in the northern regions. It contributes 203 km^3 $year^{-1}$ freshwater to the Bering Sea. It is the fifth-largest river in terms of annual total discharge in the northern regions. Hydrologic conditions and its changes in the Yukon River significantly affect regional biological and ecological systems. The US Geological Survey and Environment Canada maintain a hydrologic network in the Yukon River basin. In this study, long-term daily discharge records collected at the basin outlet station (the Pilot station, 61°56′10″N 162°53′0″W, near the river mouth) during 1975–2001 are used for analyses. Large dams and reservoirs were built in the northern regions for power generation, flood control, and irrigation. Studies show that reservoirs' regulation alters hydrologic regimes particularly in the regulated sub-basins (Ye et al. 2003; Yang et al. 2004a, b). There are no large dams in the Yukon basin; discharge data collected over this basin are reliable indicators of climate change and variation. The USGS produced a report to document the major hydrologic patterns within the basin (Brabets et al. 2000). Ge et al. (2012) examined Yukon basin hydrologic and climatic changes and variations. Yang et al. (2014b) calculated heat flux for the Yukon River.

Maps of snow extent and SWE derived from passive microwave satellite data (Scanning Multichannel Microwave Radiometer (SMMR) and Special Sensor Microwave Radiometer (SSMI)) for the Northern Hemisphere have been produced at the National Snow and Ice Data Center (NSIDC) (Armstrong and Brodzik 2001, 2002) using a modified version of the Chang et al. (1987) algorithm. The validation data set used in the Armstrong and Brodzik (2002) study was a topographically consistent subset of data from the 'Former Soviet Union Hydrological Surveys' (FSUHS) (Haggerty and Armstrong 1996). This subset (45–60 north latitude 25–45 east longitude) contains a high station density (approximately one transect per

100-km grid cell) and is primarily composed of non-complex terrain (grassland steppe) with maximum elevation differences of less than 500 m. The validation results indicated a general tendency for the algorithms to underestimate SWE in the range of 5–25 mm, particularly as forest cover density begins to exceed 30–40%. Regional maps and products have also been developed in Canada from the SMMR and SSM/I data, and used for analyses of snow cover variations over space and time (Walker and Goodison 1993; Derksen et al. 2000; Walker and Silis 2002). The algorithm by Armstrong and Brodzik (2002) is not able to consistently detect wet snow, only night time or early morning ('cold') orbits are used in most analysis, so as to reduce the chance that wet snow is present. Oelke et al. (2003) applied these SWE data for the active layer depth modeling in the Arctic and produced reasonable results. This analysis derived and applied daily SWE data for the Arctic watersheds as part of the effort to examine the large-scale seasonal and inter-annual variations of snow cover and its linkage with river flows (Yang et al. 2003, 2007).

In addition, the NOAA weekly snow cover maps based on visible data are quite reliable to map Snow Cover Extent (SCE) at many times and in many regions including the high latitudes. Mapping frequency and spatial resolution increased with the introduction of daily Interactive Multisensor Snow and Ice Mapping System (IMS) maps in June 1999. However, a lower resolution weekly map has continued to be generated from the IMS and is used in this analysis (Robinson 2003). This pseudo-weekly map involved taking high-resolution IMS grid cells for the fifth map of a week (continuing the weekly NOAA calendar) and determining whether more than 38% (determined from a comparison of both products that were produced independently during 2-year evaluation period) of the 64 IMS cells within a coarse resolution weekly cell were snow covered. If so, the coarse cell was considered snow covered (the 38% value was). Intercomparisons of visible, microwave, and station data derived weekly snow maps suggest strong agreement between the three, though admittedly lower in mountainous regions and near the periphery of the snowpack. The SCE maps have been widely used for hydrologic and climatic analyses in the cold regions, such as development of basin snow cover depletion curves (Rango 1996, 1997), study of streamflow response to snow changes in large northern rivers (Yang et al. 2003), input snow cover data to regional hydrologic and snowmelt runoff models (Rango 1997), and validation of climate model performance (Frei and Robinson 1999a; Yang et al. 1999).

This analysis used the daily EASE-Grid brightness temperature data from NSIDC (nsidc.org/data/nsidc-0032) to run the SWE algorithm (Armstrong and Brodzik 2001, 2002; Brodzik and Knowles 2002), for cold passes without the vegetation corrections, and produced daily SWE data for the northern regions including the Yukon watershed. The basin-mean SWE time-series have been generated from the daily records by averaging all pixels in the watershed. The weekly data have been generated by averaging the 7 day basin-mean SWE record during 1988–2001. On the basis of these weekly records, we examine the seasonal changes of snow cover mass, by defining the SWE climatology based on weekly statistics, determining the dates of snow cover formation/disappearance and duration of snow cover/snow-free days, and quantifying the rates of snow cover

mass change during the accumulation and melt seasons. We also derive weekly discharge time-series from the daily streamflow data collected near the basin outlet, and use the weekly data to describe the seasonal streamflow characteristics, including discharge regime, rates of streamflow rise, and peak flow during the melt period. We calculate the weekly correlation of streamflow with basin SWE, and determine the consistency between SWE and streamflow changes over the seasons. Furthermore, we identify extreme snowmelt streamflow cases and examine their correspondence with basin snow cover conditions. These analyses characterize the weekly relationship between snowmelt runoff and basin SWE changes for the Yukon River. In addition to streamflow and snow cover data, basin-mean weekly precipitation and temperature time-series during 1966–1998 have been created based on gridded global data sets (Jones 1994), and used to investigate the compatibility of SWE/SCE data with climate variables and to explain the streamflow response to seasonal snow cover changes.

It is important to note that the approach of this analysis is not a complete water budget calculation; rather, we focus on the major terms in basin water budget, i.e., SWE, winter precipitation, and streamflow. We relate snow cover data (SWE and SCE) with streamflow data measured near the basin outlet, since discharge represents the integrated response of basin hydrology to climate influence. To be compatible with discharge data, we need basin-mean snow and climate data for our analysis. To generate basin-averaged data, it is necessary to define the basin boundary. A river network grid by Fekete et al. (2001) was used over the Yukon basin and overpaid onto the gridded snow and climate data. All the grids inside the basin and those with more than 50% within the basin boundary were counted as the basin grids and used to produce basin averages. A simple average was calculated without taking into account topography effects on snow, precipitation, and temperature distributions. Similar approach has been applied for other large watersheds in North America and Siberia (Yang et al. 2003; Dyer 2008). Given the large size of the Yukon watershed and the focus of this analysis on the consistency examination of various data, the use of basin average is effective and appropriate.

9.3 Basin Hydro-Climatic Regime

To understand the climatic and hydrologic regime of the Yukon basin, we present the basin-mean temperature, precipitation, snow cover, and discharge data. The weekly timescale is used for accurate discussions of the seasonal cycles of basin hydrology and climate, particularly for snow cover and streamflow. Figure 9.2 shows the basin-mean weekly temperature regime. The basin is cold, with mean temperatures between −10 and −20 °C, during weeks 42–14; and it is relatively warm during weeks 20–38, when mean temperatures vary from 0 to 12 °C. Basin temperatures rise from −10 °C to near 0 °C during weeks 15–19, and decline from 0 to −10 °C during weeks 39–41. The inter-annual fluctuations in winter temperatures are significantly greater (ranging from −35 to −5 °C) than the differences in the

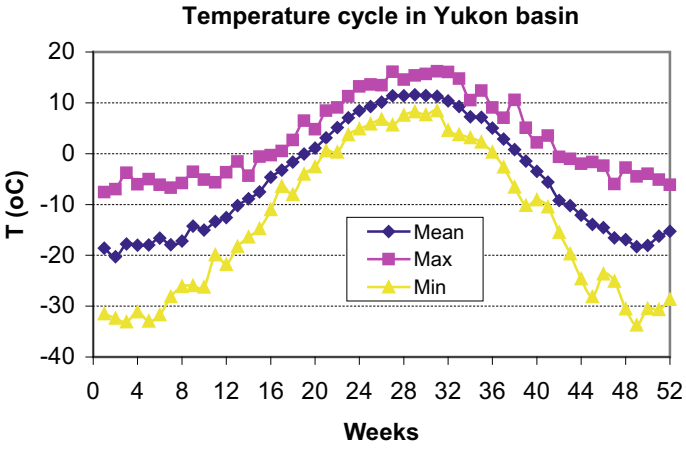

Fig. 9.2 Basin-mean weekly temperature in (T, °C) for the Yukon watershed, 1966–2002

summer temperatures (ranging from 8 to 15 °C). During the period 1966–2002, Yukon basin-mean annual air temperature is about −5.1 °C (SD = 0.98 °C), with the lowest annual air temperature of −6.8 °C in 1974, and the highest being −2.9 °C in 1993. Similar to other northern regions, Yukon basin has experienced a significant ($\alpha = 0.05$ level) warming trend (0.03 °C/year) during 1966–2002.

Similar to temperatures, a strong seasonal cycle exists for precipitation over the Yukon basin (Fig. 9.3). Precipitation is high (10–15 mm) during the warm season (weeks 21–43) and low (5–10 mm) during the winter season (weeks 44–20). During the period of 1988–2002 ($n = 15$), the mean annual total precipitation in Yukon basin is 384.6 mm (SD = 37.7 mm). The lowest annual precipitation is

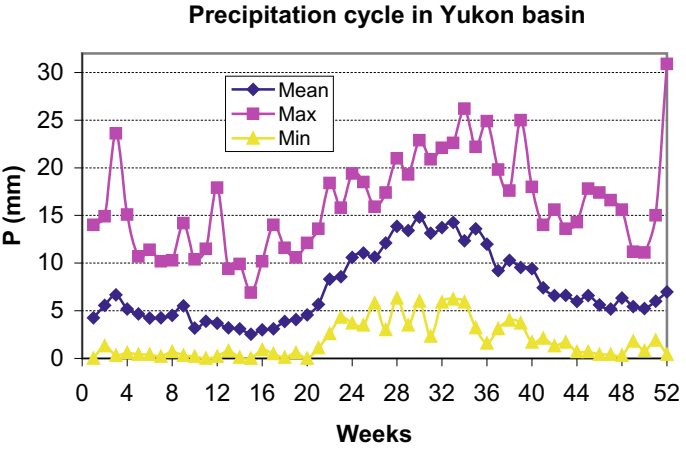

Fig. 9.3 Basin-mean weekly precipitation (P, mm) over the Yukon watershed, 1988–2002

312.3 mm in 1999, and the highest annual precipitation is 442.0 mm in 1994. The mean annual total snowfall (defined as the precipitation during the period when basin-mean air temperature is below 0 °C) is 180.4 mm (or 47% of the yearly total precipitation). The lowest annual snowfall is 102.3 mm in 1998, and the highest annual snowfall is 258.9 mm in 1992. Winter precipitation is generally lower than summer precipitation over the Yukon basin. On the 52nd week of 1999 and the 3rd week of 2000, weekly precipitation was about 31 and 24 mm, respectively; they were unusually higher for winter season perhaps due to strong snowfall events over the lower parts of the basin. No significant trends were found for yearly total precipitation and annual total snowfall for the study period 1988–2002.

Figures 9.4 and 9.5 show the basin weekly Snow Cover Percent (SCP) and SWE cycles. They illustrate snow accumulation during weeks 37–44, when basin SCE rises from 10 to 90%; a complete snow cover (100% SCE) during weeks 44–16; snowmelt during weeks 17–24, when SCE drops from 90 to 10% over the basin; and a minimum SCE of 5–10% in summer (weeks 25–36) due to glacier and snow cover in the high elevations. The SCE data show significant inter-annual variations. For the maximum SCE case, we see 100% SCE lasting during weeks 40–24, a fast melt in 2–3 weeks during weeks 25–28, a higher minimum SCE of 20–30% in the mid-summer, and an early snow accumulation during weeks 36–40. On the other hand, for the minimum SCE case, we observe a 100% snow cover during the weeks 50–16, a slow snowmelt in weeks 17–22, almost snow-free during weeks 24–39, and a late snow accumulation in weeks 40–48.

Similar pattern exists for the SWE (Fig. 9.5). Snowpack accumulates during weeks 38–4, reaches a stable state during weeks 5–16, with the mean max SWE of 90–100 mm around weeks 8–12. Snowpack starts to shrink slightly after the peak SWE. Snow cover melts during weeks 16–22, with SWE dropping from the peak to

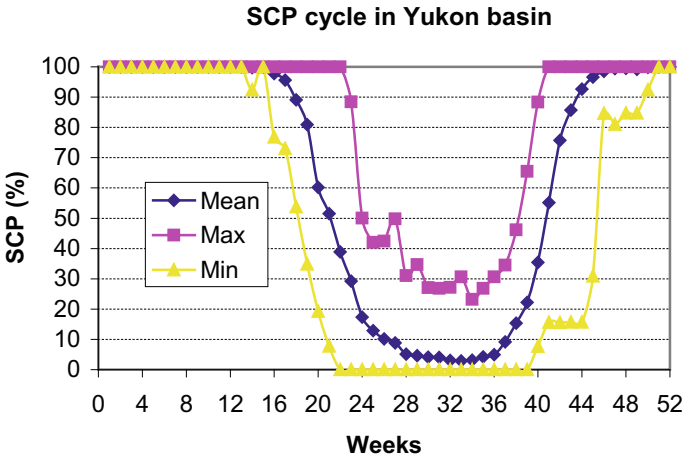

Fig. 9.4 Basin-mean weekly snow cover percentage (SCP, %) over the Yukon watershed, 1966–2002

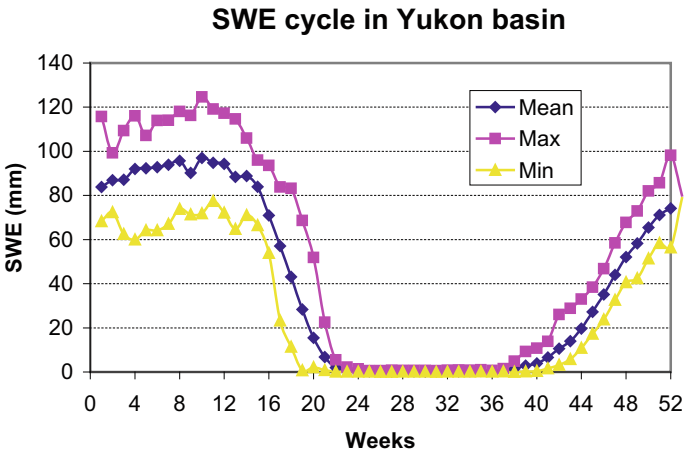

Fig. 9.5 Basin-mean weekly snow water equivalent (SWE, mm) over the Yukon watershed, 1988–2001

near 0 mm at week 23. Basin becomes snow-free during weeks 23–37, when the average SCE is about 5%, with max being as high as 30%, due to glaciers and snow cover in the high elevations. SWE condition varies among the years, for instance, the peak SWE range from 60–70 to 110–120 mm. The rate and length of snowmelt season also varies greatly, depending on the spring temperature and amount of peak SWE. A shorter melt season usually suggests a faster melt of snow cover due to late onset of melt associated with higher temperatures during late spring. During the period of 1988–2002, the mean peak SWE in Yukon basin is about 106 mm (SD = 130 mm). The lowest and highest peak SWEs are 81 mm in 1991 and 125 mm in 1998, respectively. No significant trends were found for the SCP or SWE over the study period 1988–2002.

The seasonal cycle of discharge near the basin outlet is illustrated in Fig. 9.6. It generally shows low flows during November–April (weeks 45–17), highest flow in June (weeks 22–24) due to snowmelt runoff, high flow in summer (weeks 25–40) due to glacier melt, and recession of flow in fall season (weeks 40–44). Streamflow of the Yukon River peaks at weeks 22–24 (or mid-June), when the basin is covered by a small patchy snowpack, i.e., approximately 4% SCE and 1 mm SWE over the watershed. The basin SWE amounts are very low at the time of peak streamflow, perhaps reflecting a long lag of streamflow response to snowmelt and flow routing within the large watershed. On the other hand, it should be noted that the SWE algorithm is more appropriate for the temperature gradient typical of a deep and dry snowpack. SWE will decrease in the presence of even small amount of liquid water, as soon as the cold passes start observing liquid water, since the emission from the water effectively reduces the temperature gradient. The SWE may fall off much faster than the real melt rate.

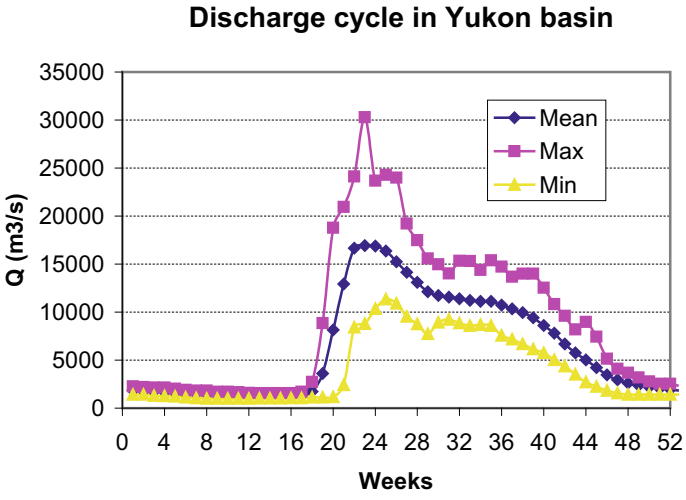

Fig. 9.6 Mean weekly discharge (m^3/s) near the basin outlet, 1975–1996

Streamflow decreases at the end of the snowmelt season, although heavy rainfall events and glacier melt in mid-summer generate secondary floods over the basin. The inter-annual variations of weekly streamflow are generally small in the cold season and large over summer months mainly due to rainfall storm activities and associated streamflow fluctuations. It also indicates noticeable differences in streamflow characteristics between years mainly due to different climate and snow conditions over the basin. The annual peak discharge in Yukon basin is 19 178 m^3/s, with the lowest and highest peak discharge being 12 969 m^3/s in 1978, and 30 299 m^3/s in 1985, respectively. It is important to note that the year having the highest annual flow was the same year for the highest peak flow, and the year with the lowest annual flow also has the lowest peak flow. This indicates that the peak flow in spring and summer dominates the annual flow. No significant changes were found for peak discharge or annual total discharge during the study period.

9.4 Compatibility of Basin Snow Cover Data

Temperature and precipitation are the main factors affecting snow cover characteristics including accumulation and melt processes. To understand the winter snow-mass budget, we compare basin SWE with the Accumulated Precipitation (AP) over the period when the basin-mean weekly temperatures are below 0 °C. The AP may include some rainfall events in early spring and late fall seasons particularly over the southern parts of the watersheds. The contribution of rainfall events is small to the winter total precipitation.

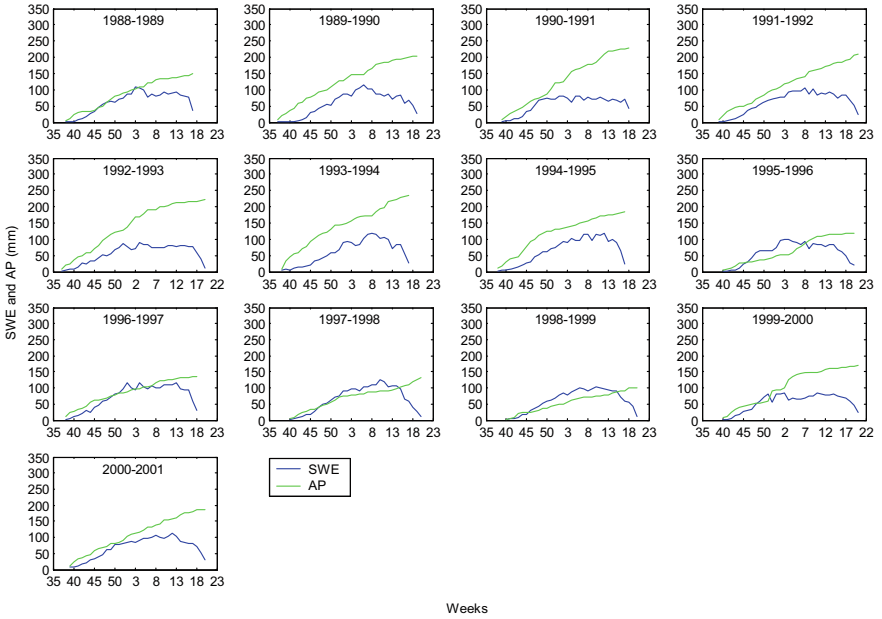

Fig. 9.7 Comparisons of basin snow water equivalent (SWE, mm) with winter Accumulated Precipitation (AP, mm) from 1988/1989 to 2000/2001 (Zhao 2004)

Figure 9.7 shows significant variation in the AP among the years. Both the high and low AP winters were associated with similar SWE amounts, although in most years basin SWE is generally less than the AP during the snow cover season. It is interesting to note that the amounts of maximum SWE are closer to AP in low snowfall winters, and much less than AP in high snowfall winters. These results are consistent with the saturation in the temperature gradient with the modeling work by Chang et al. (1987). It is reasonable to expect that basin maximum SWE should be generally close to winter total snowfall amount. The lack of correspondence of the basin SWE to AP variation indicates some inconsistency between the SWE and precipitation data. This is not completely unexpected given the large biases in snowfall data over the high-latitude regions (Yang et al. 1998, 2005; Yang and Ohata 2001) and limitations in remote sensing snow cover algorithm, including the issue of saturation (Walker and Goodison 1993; Armstrong and Brodzik 2001). In addition, sublimation loss from snowpack over winter is another factor contributing to the uncertainty in SWE and AP compatibility. As discussed in Chaps. 3 and 4, many studies reported that sublimation from the snow surface accounts for up to 1/3 of total accumulation in the northern regions (Benson 1982; Liston and Sturm 1998, 2004). Sublimation over large basins and regions is difficult to determine through direct measurements. Snow models taking into account the blowing and drifting snow processes can provide reasonable estimate of regional winter sublimation

amount (Liston and Sturm 1998, 2002). The ratios of maximum basin SWE versus AP are 37–120% (mean 77%) for the Yukon River. The ratios close to 100% reflect less difference between the SWE and AP.

The inter-annual variations in the SWE/AP ratios are mainly due to fluctuations in snowfall amounts and temperatures over the winter season. The low (high) ratios are found associated with high (low) AP and warm (cold) winter. It is important to note that the Yukon basin SWE was greater than the AP for several winters (i.e., 1995–1996, 1996–1997, 1997–1998, and 1998–1999). This unexpected result indicates uncertainties in the SWE and AP estimations over the region. There might be possible SWE algorithm saturation, as the basin-average SWE never exceeded 100 mm, regardless of winter precipitation variation. In addition, precipitation gauge undercatch of snowfall is also a factor, since studies (Yang et al. 1998, 2005; Benning and Yang 2005) found underestimation of yearly precipitation by 25–50% over Alaska. In addition, determination of timing of snow cover accumulation is also a challenge. In this analysis, basin-mean temperatures at 0 C were used to estimate the beginning date (week) of snow cover formation, i.e., the starting point for AP. Given the very large size of the watershed, basin-mean temperatures do not always represent the thermal conditions over the entire basin, particularly during spring and fall transition periods. Sub-basin scale analyses might be necessary to better examine the compatibility between basin SWE and winter precipitation.

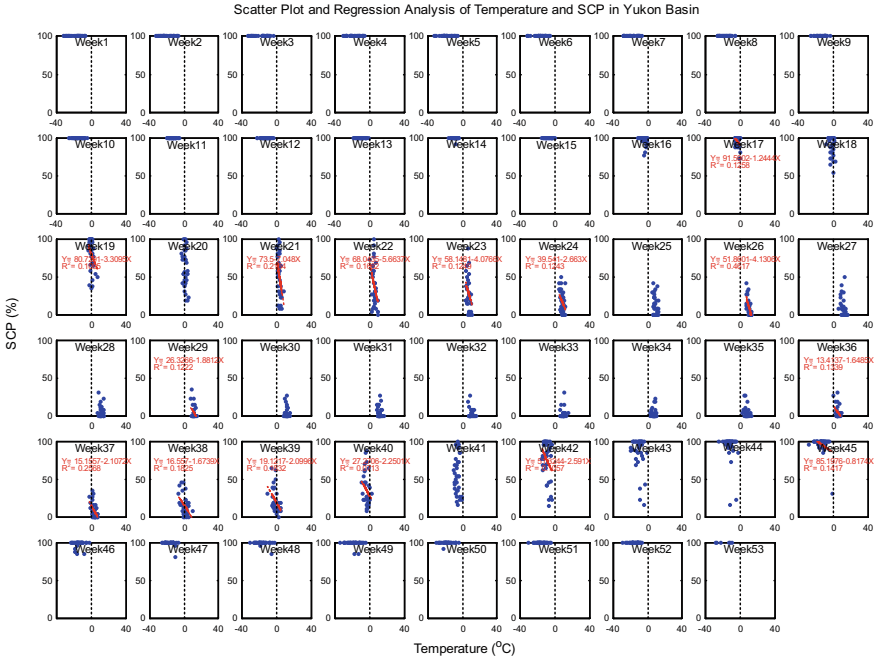

Fig. 9.8 Scatter plots and regression equations of basin weekly SCP (%) versus weekly air temperature (°C) for the 53 weeks in a year during 1966–2001 (Zhao 2004)

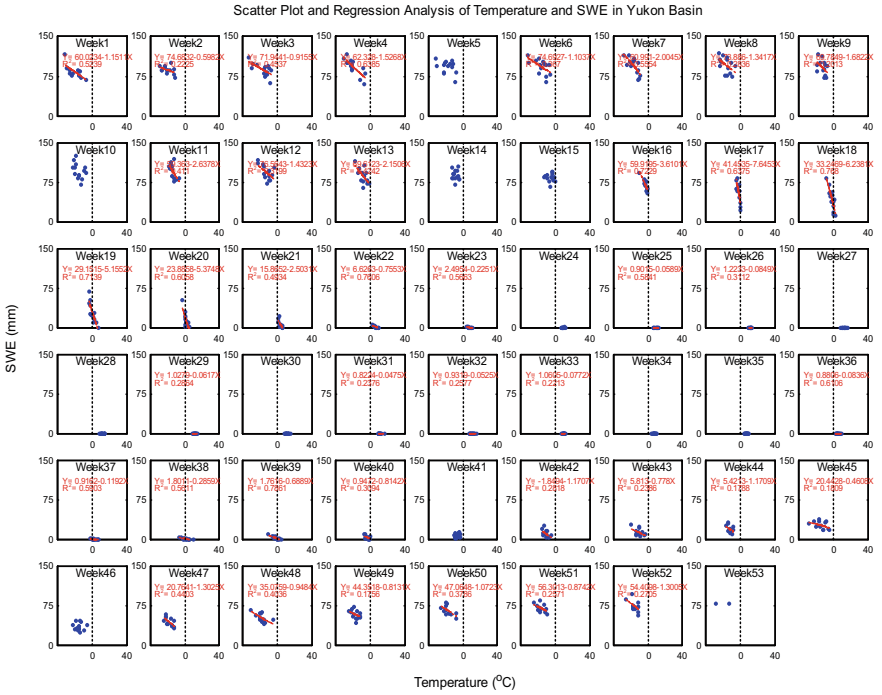

Fig. 9.9 Scatter plots and regression equations of basin weekly SWE (mm) versus weekly air temperature (°C) for the 53 weeks in a year during 1988–2001 (Zhao 2004)

To examine and quantify the impact of temperature on basin snow cover conditions, a linear regression is applied to the temperature and SCE/SWE data sets for each week in a year. Figures 9.8 and 9.9 present the scatter plots of (snow cover percent or SCE) SCP versus temperature and SWE versus temperature for the 53 weeks. The regression functions and R^2 are displayed in the plots for the weeks with significant relationships. The results generally show that the snow cover changes as a function of temperature. The basin SCP and SWE are the highest in the beginning of the year when temperatures are very cold between −15 and −20 C. Both SCP and SWE decrease in spring from very high to very low in a short time period when basin-mean temperatures are around 0 C. The basin is almost snow-free in the short summer season except in the mountain regions with glaciers and snow cover all year around. Snow cover forms when temperatures drop back to around 0 C in fall and continues to accumulate over the fall–winter seasons. Regression analyses identify strong negative correlations between basin SCP/SWE and temperature, particularly when temperatures are close to 0 C during the snow accumulation and melt seasons (Figs. 9.8 and 9.9). These correlations demonstrate the association of (high) low SWE/SCP with (low) high temperatures.

9.5 Weekly Relation Between Streamflow and Basin SWE

The seasonal changes of the basin SWE and streamflow in each individual year are displayed in Fig. 9.10. They clearly indicate a general response of river runoff to seasonal snow cover changes, i.e., an association of high discharge with low SCE and SWE during summer, a decrease in discharge associated with increasing SCE and SWE in fall, an association of low streamflow with high SCE and SWE during the cold season, and an increase in discharge associated with decreasing SCE and SWE during the spring melt periods. They also show the inter-annual variations in both SWE and streamflow. Relative to the basin SWE, streamflow varies much more between years. For instance, the Yukon River peak streamflow was high (23 000 m^3/s) in 1991 and low (18 000 m^3/s) in 1996, while the maximum basin SWE was low (about 75 mm) in 1991 and high (about 90 mm) in 1996. A similar peak SWE was found for 1988, 1989, 1990, 1994, 1995, and 2001, while the spring peak flow differs significantly among these years, particularly between 1994 (low flow) and 2001 (high flow). This discrepancy between basin snow cover and streamflow variations may suggest uncertainties in basin SWE data perhaps due to algorithm limitations (Armstrong and Brodzik 2002), particularly for the mountain regions within the Yukon basin.

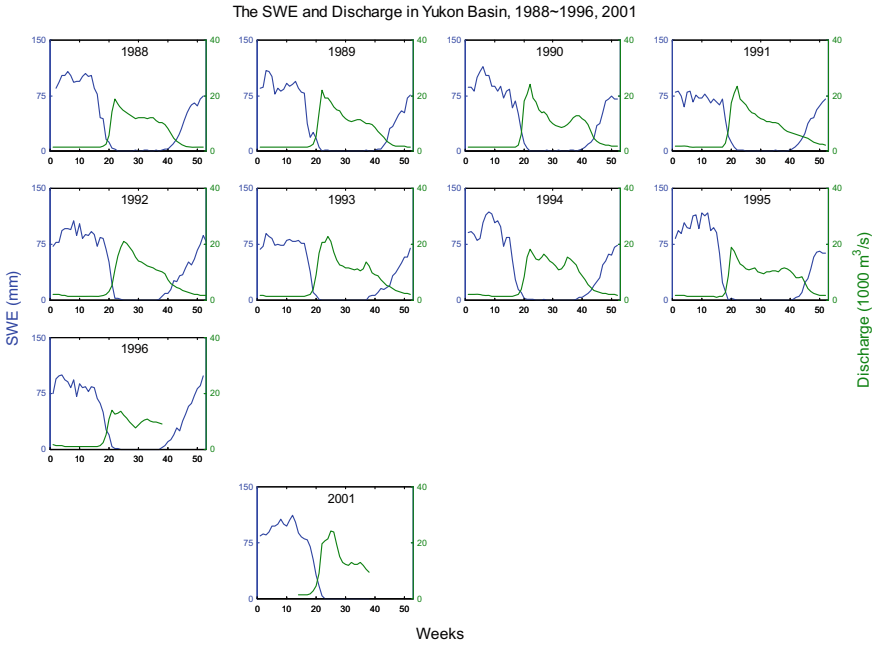

Fig. 9.10 Comparisons of basin Snow Water Equivalent (SWE, mm) with river discharge (Q, m^3/s) during 1988–1996 and 2001 (Zhao 2004)

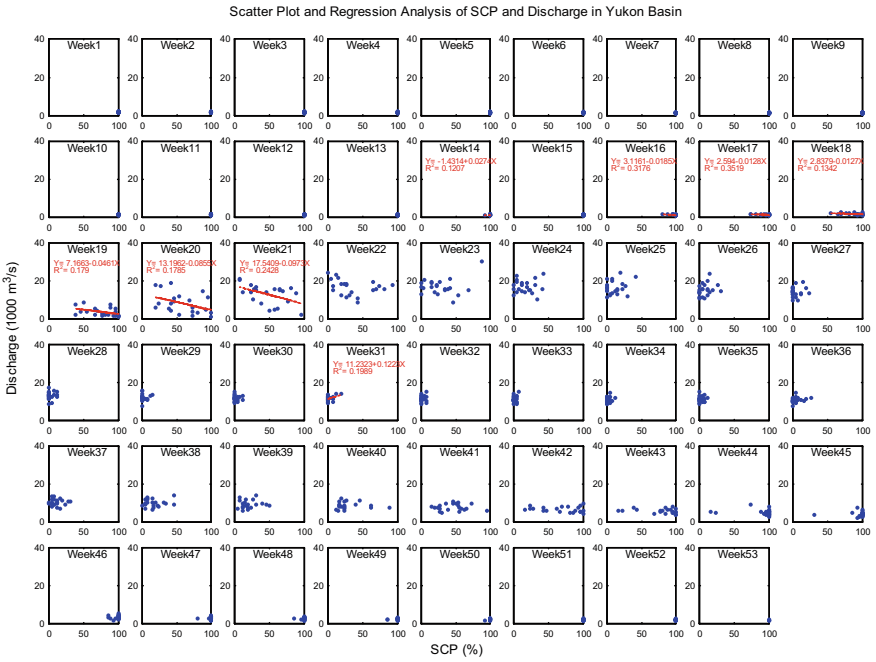

Fig. 9.11 Scatter plots and regression equations of weekly discharge (Q, m^3/s) versus weekly basin Snow Water Equivalent (SWE, mm) for the 53 weeks in a year, 1988–2001 (Zhao 2004)

To quantify the response of river streamflow to basin snow cover variation, we examine and compare the weekly mean streamflow with the weekly basin SWE for the study period 1988–1999. The results generally confirm a meaningful relationship between the streamflow and SWE during the spring melt season over the Yukon watershed (Fig. 9.11). In the early melt period (weeks 16–18), basin SWE reduces from 120 to 50 mm. Most of the meltwater is stored in ponds, lakes, and river valleys. River ice breaks up around this time in the upper parts of the basin, but streamflow at the basin outlet does not show a clear response due to ice jams in the river valleys. As snowmelt progresses (weeks 19–21), SWE decreases from 70 to 20 mm, releasing more water to satisfy the surface storage within the basin. During weeks 22–24, river channels open up in the downstream parts of the watershed and discharge near the basin mouth starts to rise and reach the maximum. This response of streamflow to snowmelt is reflected by a negative correlation between streamflow and basin SWE in weeks 19–21. In the late melt period (weeks 23–25), streamflow response to snowmelt weakens due to reduced snowmelt runoff contribution. The results of regression analyses are shown in Fig. 9.11. They explain 30–70% of streamflow variability, although they are statistically significant at 85–95% confidence. It is useful to derive these relationships, as they suggest a practical procedure of using remotely sensed SWE information for snowmelt runoff estimation over the large northern watersheds.

9.6 Extreme Streamflow and Associated Snow Condition

The basin snow cover and discharge data show that weekly snow cover and snowmelt peak flows vary significantly among years. To better understand the variability in snowmelt runoff, it is useful to examine extreme streamflow and its association with the snow cover condition, such as the peak accumulation and melt process. Two sample years of highest and lowest streamflow cases were selected, i.e., peak flows during the snowmelt season of 13 900 m^3/s in 1996 and 24 110 m^3/s in 1990. Figure 9.12 compares the SCE and SWE data with the extreme streamflow for the two years. It shows that, for the SCE, a similar process (rate) of snow cover depletion during the early melt season (weeks 17–20) between the two years, and a slower melt and longer SCE recession for the low flow year during the late melt season (weeks 21–25) (Fig. 9.12a). The peak snow accumulation over the basin is about 115 mm for the high flow year of 1990 and 100 mm for the low flow year of 1996, indicating higher (lower) flows associated with higher (lower) basin SWE. The melt patterns were very similar between the two extreme years, with the snowmelt beginning around week 16 and ending around week 21. The timing of the peak flow was 1 week earlier in the low flow year than the high flow year; the shape of the spring hydrograph is sharp (with a single high peak) in the high flow year and flat (with two low peaks) in the low flow year. It is important to note that the difference in peak SWE was only 15 mm, while the peak spring flow difference was about 10 210 m^3/s (Fig. 9.12b). The difference in peak flows is much higher than the difference in basin SWE between the extreme years. This seems to suggest inconsistency between basin SWE and streamflow. In addition to the winter maximum SWE over the basin, other factors such as temperature, precipitation, soil moisture condition, and ground thaw processes during the melt periods also affect snowmelt processes and influence the timing and magnitude of peak snowmelt floods.

9.7 Summary and Conclusion

Validation and evaluation of available remotely sensing products are important to develop our capability of observing and monitoring the earth system from the space. This analysis applied remotely sensed SWE, SCE, and gridded climatic data to investigate snowmelt runoff response to seasonal snow cover change over the Yukon watershed. It defined the seasonal cycles and variations of snow cover and river streamflow, and identified a clear correspondence of river streamflow to seasonal snow cover change, i.e., an association of low streamflow with high snow cover mass during the cold season and an increase in discharge associated with a decrease of snow cover extent and SWE during the melt periods. It also examined the compatibility of the basin SWE data with the SCE, peak snowmelt floods, and climatic variables (temperature and winter precipitation), and found consistency among the basin SWE, SCE, and temperature. On the other hand, it detected

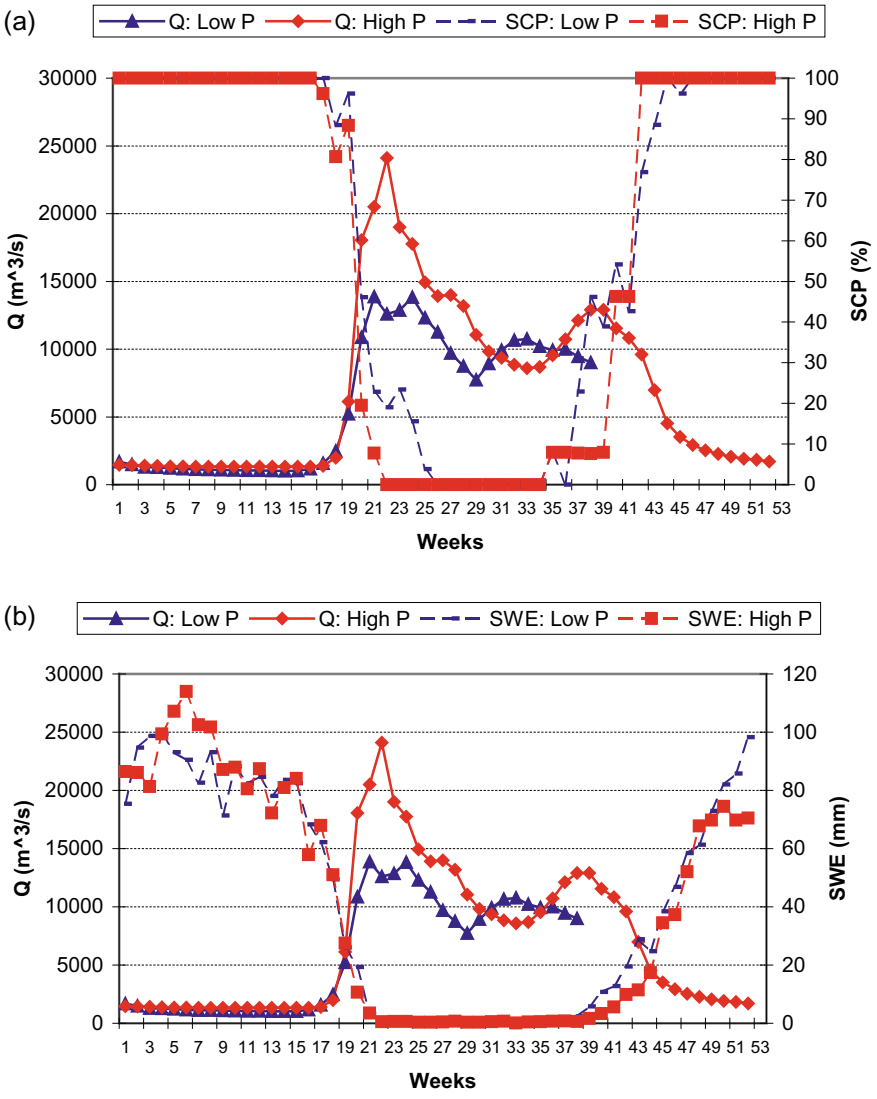

Fig. 9.12 Comparison of extreme discharge (Q, m^3/s) cases with SCP (**a**) and SWE, (**b**) over the Yukon watershed (Zhao 2004)

incompatibility between basin SWE and winter precipitation, suggesting limitations in SWE retrieval algorithm and uncertainties in the determination of basin winter snowfall amounts.

To quantify the relation between river streamflow and basin snow cover variations, we compared the weekly mean streamflow with the weekly basin SWE for the study period. The results revealed a meaningful linkage between streamflow and

basin SWE during the spring melt season, and developed a statistically significant weekly streamflow–SWE relationship. It is important to explore these relationships, as they improve our understanding of the most important arctic hydrologic process —snowmelt peak floods—and they also suggest practical procedures of using remotely sensed snow cover information for snowmelt runoff forecasting over the large northern watersheds with insufficient ground observations. Furthermore, analyses of extreme (high/low) streamflow cases (years) and basin snow cover conditions indicate a general association of high (low) flow peak with high (low) maximum SWE over the basin, although some inconsistencies exist between extreme flow and basin SWE. These results point to a need to further search for the best snowmelt–streamflow relationship, and to develop the most useful snowmelt runoff forecasting methods for the large northern rivers. There are uncertainty and saturation problems in the SWE algorithms (Clifford 2010). There is good improvement in passive microwave SWE algorithms, including the AMSR-E (Kelly 2009; RSSJ) that includes adjustments for shallow show and a dynamic density model.

The results of this analysis demonstrate that remote sensing snow cover data are useful in understanding streamflow characteristics and changes in the arctic regions with a very sparse observational network. The methods and results of this investigation are important to seasonal hydrologic forecasting, snowmelt model, and process studies. They improve our understanding of the spatial and temporal variability of high-latitude snow cover and its contribution to river runoff in the northern rivers. Snow depth and water equivalent data obtained by ground observations are also useful to better understand snowmelt and runoff processes (Dyer 2008; Brown et al 2010). Long-term snow observations particularly over the Siberian regions have been found valuable for cold region climate studies (Ye et al. 1998; Armstrong and Brodzik 2001). There is a need to investigate the compatibility of the SWE with in situ snow cover observations at sub-basins scales for more detailed analyses of snow–runoff relationship. It is also necessary to integrate remote sensing and ground-based snow datasets for land surface process modeling and simulation of hydrologic change over the cold regions.

References

Aagaard K, Carmack EC (1989) The role of sea ice and other fresh water in the arctic circulation. J Geophys Res 94(C10):14485–14498

Armstrong RL, Brodzik MJ (2001) Recent Northern Hemisphere snow extent: a comparison of data derived from visible and microwave sensors. Geophys Res Lett 28(19):3673–3676. https://doi.org/10.1029/2000GL012556

Armstrong RL, Brodzik MJ (2002) Hemispheric-scale comparison and evaluation of passive microwave snow algorithms. Ann Glaciol 34:38–44

Benning J, Yang D (2005) Adjustment of daily precipitation data at Barrow and Nome Alaska for 1995–2001. Arct Antarct Alp Res 37(3):267–283

Benson CS (1982) Reassessment of winter precipitation on Alaska's Arctic Slope and measurement on the flux of wind blown snow report. Geophysical Institute of the University of Alaska, Fairbanks, AK, p 26

Brabets T, Wang B, Meade R (2000) Environmental and hydrologic overview of the Yukon river basin, Alaska and Canada, USGS. Water-Resour Investig Rep 99–4204:106

Brodzik MJ, Knowles KW (2002) EASE-grid: a versatile set of equal-area projections and grids. In: Goodchild M (ed) Discrete global grids. National Center for Geographic Information & Analysis, Santa Barbara, CA. http://www.ncgia.ucsb.edu/globalgrids-book/ease grid/

Brown R, Brasnett B, Robinson D (2010) Gridded North American monthly snow depth and snow water equivalent for GCM evaluation. Atmos Ocean. https://doi.org/10.3137/ao.410101

Cao Z, Wang M, Proctor B, Strong G, Stewart R, Ritchie H, Burnford J (2002) On the physical processes associated with the water budget and discharge of the Mackenzie basin during the 1994/95 water year. Atmos Ocean 40(2):125–143

Chang ATC (1997) Snow parameters derived from microwave measurements during the BOREAS winter field campaign. J Geophys Res 102(D24):29663–29671

Chang ATC, Foster JL, Hall DK (1987) Nimbus 7 SMMR derived global snow cover parameters. Ann Glaciol 9:39–44

Clark MP, Serreze MC, Robinson DA (1997) Atmospheric controls on Eurasian snow extent. Int J Climatol 19(1):27–40

Clifford D (2010) Global estimates of snow water equivalent from passive microwave instruments: history, challenges and future developments. Int J Remote Sens 3707–3726. https://doi.org/10.1080/01431161.2010

Derksen C, LeDrew E, Goodison B (2000) Temporal and spatial variability of North American prairie snow cover (1988–1995) inferred from passive microwave-derived snow water equivalent imagery. Water Resour Res 36(1):255–266

Dyer JL (2008) Snow depth and streamflow relationships in large North American watersheds. J Geophys Res 113:D18113. https://doi.org/10.1029/2008JD010031

Dyer JL, Mote TL (2006) Spatial variability and trends in snow depth over North America. Geophys Res Lett 33:L16503. https://doi.org/10.1029/2006GL027258

Fekete BM, Vörösmarty CJ, Lammers RB (2001) Scaling gridded river networks for macroscale hydrology: development, analysis, and control of error. Water Resour Res 37(7):1955–1967

Frei A, Robinson DA (1999a) Northern Hemisphere snow extent: regional variability 1972–1994. Int J Climatol 19(14):1535–1560

Frei A, Robinson DA (1999b) Evaluation of snow extent and its variability in the atmospheric model intercomparison project. J Geophys Res 103(D8):8859–8871

Ge S, Yang D, Kane D (2012) Yukon river basin long-term (1977–2006) hydrologic and climatic analysis. Hydrol Process. https://doi.org/10.1002/hyp.9282

Haggerty CD, Armstrong RL (1996) Snow trends within the Former Soviet Union. Eos 77(46): [Abstract] Fall Meeting Supplement, F191

Jones PD (1994) Hemispheric surface air temperature variations: a reanalysis and an update to 1993. J Clim 7:1794–1802

Kane DL (1997) The impact of Arctic hydrologic perturbations on Arctic ecosystems induced by climate change. In: Global change and Arctic terrestrial ecosystems, ecological studies, vol 124. Springer, New York, pp 63–81

Kane DL, Hinzman LD, McNamara JP, Zhang Z, Benson CS (2000) An overview of a nested watershed study in Arctic Alaska. Nord Hydrol 4(5):245–266

Kelly REJ (2009) The AMSR-E snow depth algorithm: description and initial results. J Remote Sens Soc Jpn 29(1):307–317. (GLI/AMSR Special Issue)

Lammers R, Shiklomanov A, Vorosmarty C, Fekete B, Peterson B (2001) Assessment of contemporary arctic river runoff based on observational discharge records. J Geophys Res 106 (D4):3321–3334

Liston GE, Sturm M (1998) A snow-transport model for complex terrain. J Glaciol 44:498–516

Liston GE, Sturm M (2002) Winter precipitation patterns in Arctic Alaska determined from a blowing-snow model and snow-depth observations. J Hydrometeorol 3:646–659

Liston GE, Sturm M (2004) The role of winter sublimation in the Arctic moisture budget. Nord Hydrol 35(4):325–334

Oelke C, Zhang T, Serreze MC, Armstrong RL (2003) Regional-scale modeling of soil freeze/thaw over the Arctic drainage basin. J Geophys Res 108(D10):4314. https://doi.org/10.1029/2002JD002722

Rango A (1996) Spaceborne remote sensing for snow hydrology applications. Hydrol Sci J 41 (4):477–494

Rango A (1997) Response of areal snow cover to climate change in a snowmelt-runoff model. In: Walsh JE (eds) International symposium on representation of the cryosphere in climate and hydrological models, vol 25, Victoria, British Columbia. Annals of Glaciology, Cambridge, UK, pp 232–236

Rango A, Shalaby AI (1999) Current operational applications of remote sensing in hydrology. Operational hydrology report, No. 43. World Meteorological Organization (WMO), Geneva, p 73

Robinson DA (1989) Construction of a United States historical snow data base. In: Proceedings of eastern snow conference, vol 45, pp 50–59

Robinson DA (2003) Recent variability of Northern Hemisphere snow cover. In: Preprints: seventh conference on polar meteorology and oceanography, paper 13.12. American Meteorological Society, Hyannis, MA, p 6

Robinson DA, Frei A (2000) Seasonal variability of Northern Hemisphere snow extent using visible satellite data. Prof Geogr 52(2):307–314

Robinson DA, Dewey KF, Heim RR Jr (1993) Global snow cover monitoring: an update. Bull Am Meteor Soc 74:1689–1696

Serreze MC, Maslanik JA, Scharfen G, Barry RG (1993) Interannual variations in snow melt over arctic sea ice and relationships to atmospheric forcings. In: Proceedings of the 3rd international symposium on remote sensing of snow and ice, vol 17. Annals of Glaciology, Boulder, CO, pp 327–331

Serreze MC, Walsh JE, Chapin EC, Osterkamp T, Dyugerov M, Romanovsky V, Oechel WC, Morison J, Zhang T, Barry RG (2000) Observation evidence of recent change in the northern high-latitude environment. Clim Change 46:159–207

Serreze MC, Bromwich DH, Clark MP, Etringer AJ, Zhang T, Lam-mers RB (2002) The large scale-hydro-climatology of the terrestrial arctic drainage system. J Geophys Res 107:8160. https://doi.org/10.1029/2001JD000919

Walker AE, Goodison BE (1993) Discrimination of a wet snow cover using passive microwave satellite data. Ann Glaciol 17:307–311

Walker AE, Silis A (2002) Snow-cover variations over the Mackenzie River basin, Canada, derived from SSM/I passive-microwave satellite data. Ann Glaciol 34:8–14

Whitfield P, Cannon A (2000) Recent climate moderated shifts in Yukon hydrology. Water resources in extreme environments, AWRA. Anchorage, Alaska, pp 257–262

Woo M-K (1986) Permafrost hydrology in North America. Atmos Ocean 24(3):201–234

Yang D, Ohata T (2001) A bias corrected Siberian regional precipitation climatology. J Hydrometeorol 2(1):122–139

Yang D, Goodison BE, Benson CS, Ishida S (1998) Adjustment of daily precipitation at 10 climate stations in Alaska: application of WMO intercomparison results. Water Resour Res 34(2):241–256

Yang ZL, Dickinson RE, Hahmann AN, Niu G-Y, Shaikh M, Gao X, Bales RC, Sorooshian S, Jin J (1999) Simulation of snow mass and extent in general circulation models. Hydrol Process 13(12/13):2097–2113

Yang D, Kane D, Hinzman L, Zhang X, Zhang T, Ye H (2002) Siberian Lena river hydrologic regime and recent change. J Geophys Res 107(D23):4694. https://doi.org/10.1029/2002JD00254

Yang D, Robinson D, Zhao Y, Estilow T, Ye B (2003) Streamflow response to seasonal snow cover extent changes in large Siberian watersheds. J Geophys Res 108(D18):4578. https://doi.org/10.1029/2002JD003149
Yang D, Ye B, Kane D (2004a) Streamflow changes over Siberian Yenisei river basin. J Hydrol 296:59–80
Yang D, Ye B, Shiklomanov A (2004b) Streamflow characteristics and changes over the Ob river watershed in Siberia. J Hydrometeorol 5(4):595–610
Yang D, Kane D, Zhang Z, Legates D, Goodison B (2005) Bias-corrections of long-term (1973–2004) daily precipitation data over the northern regions. Geophys Res Lett 32:L19501. https://doi.org/10.1029/2005GL024057
Yang D, Zhao Y, Armstrong R, Robinson D, Brodzik M-J (2007) Streamflow response to seasonal snow cover mass changes over large Siberian watersheds. J Geophys Res 112:F02S22. https://doi.org/10.1029/2006jf000518
Yang D, Shi X, Marsh P (2014a) Variability and extreme of Mackenzie River daily discharge during, 1973–2011. Quat. Int. https://doi.org/10.1016/j.quaint.2014.09.023
Yang D, Marsh P, Ge S (2014b) Heat flux calculations for Mackenzie and Yukon Rivers. Polar Sci. https://doi.org/10.1016/j.polar.2014.05.001
Ye H, Cho H, Gustafson PE (1998) The changes in Russian winter snow accumulation during 1936–1983 and its spatial patterns. J Clim 11:856–863
Ye B, Yang D, Kane D (2003) Changes in Lena river streamflow hydrology: human impacts versus natural variations. Water Resour Res 39(8):1200. https://doi.org/10.1029/2003WR001991
Zhang T (2005) Influence of the seasonal snow cover on the ground thermal regime: an overview. Rev Geophys 43:RG4002. https://doi.org/10.1029/2004RG000157
Zhang T, Barry RG, Knowles K, Heginbottom JA, Brown J (1999) Statistics and characteristics of permafrost and ground-ice distribution in the Northern Hemisphere. Polar Geogr 23(2):132–154
Zhang X, Harvey KD, Hogg WD, Yuzyk TR (2001) Trends in Canadian streamflow. Water Resour Res 37:987–998
Zhao Y (2004) Snow runoff assessment for five large northern watersheds. MS thesis. University Alaska Fairbanks

Dr. Daqing Yang is a Research Scientist at the Watershed Hydrology and Ecology Research Division, Environment and Climate Change Canada. He is also Affiliate Research Professor at the International Arctic Research Center, Univ. of Alaska Fairbanks. Over the past 25 years, he has conducted cryosphere system research in China, Canada, Japan, USA, and Norway. His primary research activities/interests include cold region hydrology and climate, particularly Arctic large river streamflow regime and change, snow cover and snowfall measurements, climate change and human impact to regional hydrology, and applications of remote sensing in cold regions. He has served as journal editor and subject editor for IAHS publications (cold region hydrology, northern research basin water balance, and cold/mountain region hydrological systems under climate change), and WMO technical reports (solid precipitation measurement intercomparison and integrated global observing strategy cryosphere theme). He also contributed as review and/or author to the IPCC Reports, and the Arctic Council's Snow, Water, Ice and Permafrost in the Arctic

(SWIPA 2017 and follow up) assessment. His current research focuses on investigating the impacts of climate variability/change and human activities on hydrologic system across the broader northern regions.

Yuanyuan Zhao P.E., is a civil engineer and a resident of Fairbanks Alaska. Her research interests are varied; she has studied streamflow response to snow cover changes in large northern river watersheds in the early 2000s for her graduate study in hydrology. She also conducted analysis of Alaska oil production cycles in resource economics. Currently, she is pursuing a Ph.D. in mathematics, studying control, and inverse problem on quantum graphs. She is a recipient of the National Science Foundation Graduate Study Fellowship.

Dr. Richard L. Armstrong is a Senior Research Scientist at the National Snow and Ice Data Center (NSIDC), Associate Professor (Adjunct) at Department of Geography, Associate Director for the Cryospheric and Polar Processes Division, and Council of Fellows of the Cooperative Institute for Research in Environmental Sciences (CIRES), University of Colorado in Boulder. His research has covered a variety of relevant topics, including (1) evaluation of fluctuations of glaciers and seasonal snow cover as indicators of climate change, (2) assessments of the individual contribution of melting seasonal snow and glacier ice to the water resources of high mountain basins, (3) passive microwave satellite remote sensing of snow, ice and frozen ground, (4) validation and cross-calibration of satellite sensor data to assure quality time series data in support of accurate climate change detection, (5) former director of various relevant field projects including Blue Glacier Mass Balance Project, Mount Olympus, University of Washington and San Juan Avalanche Project, San Juan Mountains, University of Colorado. He is also the Principal Investigator for the USAID-funded CHARIS project (Contribution to High Asian Runoff from Ice and Snow) 2013–2019.

Dr. Mary J. Brodzik received the B.A. (summa cum laude) degree in mathematics from Fordham University, New York, NY, USA, in 1987. Her experience includes software development, validation, and verification on Defense Department satellite command and control, and satellite tracking systems. Since 1993, she has been with the National Snow and Ice Data Center (NSIDC) and with the Cooperative Institute for Research in Environmental Sciences, University of Colorado, Boulder, CO, USA, where she is currently a Senior Associate Scientist. At NSIDC, she has implemented software systems to design, produce, and analyze snow and ice data products from satellite-based visible and passive microwave imagery. She has contributed to the NSIDC data management and software development teams for the NASA Cold Lands Processes Experiment and Operation IceBridge. She is managing the operational production of the EASE-Grid 2.0 Earth Science Data Record of satellite passive microwave data, including over 100 years of observations from SMMR, SSM/I-SSMIS, AMSR-E, and SMAP. She is currently working to produce enhanced-resolution, near real-time snow water equivalent products. She has used MODIS snow products to derive the first systematically derived global map of the world's glaciers. She has developed snow and glacier ice melt models to better understand the contribution of glacier ice melt to major rivers with headwaters in High Asia. Her research interests include optical and passive microwave sensing of snow, remote sensing data gridding schemes, and effective ways to visualize science data. She is a member of IEEE and the IEEE Geoscience and Remote Sensing Society.

Dr. David Robinson is a Distinguished Professor in the Department of Geography at Rutgers, The State University of New Jersey, and also the New Jersey State Climatologist. As a physical geographer and climatologist, his research interests run the spatial gamut from global to local, with an underlying theme being the development of a better understanding of the climate system. The majority of his published research has focused on hemispheric and regional snow cover dynamics and interactions of snow cover with other climate elements. This includes maintaining an internationally recognized database of Northern Hemisphere snow extent throughout the satellite era; information that is used in his Global Snow Lab's research endeavors, efforts of others, and contributions to national and international climate assessments. He has been a member of the National Academy of Sciences' Board on Atmospheric Sciences and Climate, is past president of the American Association of State Climatologists, is a Fellow of the American Meteorological Society, and has received the Lifetime Achievement award of the American Association of Geographers.